MGPB

Effects of a pillarless, center-out stoping pattern on haulage drift performance and ore tonnage at risk

Rudarsko-geološko-naftni zbornik
(The Mining-Geology-Petroleum Engineering Bulletin)
UDC: 622.3
DOI: 10.17794/rgn.2022.2.8

Original scientific paper

Wael R. Abdellah
Mining & Metallurgical Eng. dept., Faculty of Engineering, University of Assiut, Egypt, 71515, Egypt,
ORCID: https://orcid.org/0000-0001-8133-7817

Abstract

With respect to mining sequence, this article intends to investigate the impact of pillarless centre-out stoping patterns (e.g. pyramidal sequences) on the performance of mine haulage drifts (e.g. ore access units), the tonnage of unmined ore at risk, and the required quantity of fill material. Using RS²D software, a two-dimensional, elasto-plastic finite-element model for a haulage drift located at 1200m below the surface in the orebody's footwall has been built. The spread of yielding zones into the rock mass around an access drift and unmined stopes is used to assess mine haulage drift stability and estimate the amount of unmined ore at risk owing to local mining activity. The findings are presented and discussed in terms of the size of failure zones, the number of tonnes of unmined blocks at risk, and the amount of backfill materials required, all in relation to the mining stage. The findings show that haulage drift stability is rapidly diminishing. The drift roof begins to deteriorate at an early stage (after mining step 3). In the drift roof, left wall, floor, and right wall, failure zones measured 1.55m (step 3), 2.28m (step 4), 2.57m (step 5) and 1.88m (step 5) accordingly. After mining step 4, there was a total of 905 m³ of unmined ore at risk (4100 tons), and after mining step 5, a total of 1500 m³ (30 tons) of back fill material was required to strengthen stopes.

Keywords:
haulage drift stability; ore at risk; quantity of backfill; pillarless, centre-out-stoping system; yielding zone

1. Introduction

An engineering issue arises in the form of mine layout, ore body sequencing, and ground control practice in ensuring economic viability and acceptable safety at the mine's existing depth, and with deeper mine development. This necessitates knowledge of the expected behaviour of the rock mass, as well as failure mechanisms and damage (**Yao et al., 2014**; **De Santis et al., 2019**; **Forbes et al. 2020**). The planning of an underground mine has significant challenges in terms of safety, environmental protection, ground control, and production scheduling. An integrated optimal stope plan and production schedule is necessary to coordinate underground mining activities, such as development, extraction, haulage, dumping, stockpiling, and processing in order to maximize the profitability of these operations (**Brickey, 2015**; **Carpentier et al. 2016**; **Appianing and Ben-Awuah, 2018**; **Wu, 2020**). Different mining patterns could be used to obtain the tabular ore deposit (e.g. primary-secondary stoping, pillarless centre-out stoping, etc.). Such patterns have an impact on the mining environment in terms of rock mass behaviour, stress distribution, orezone access unit serviceability, and stope extraction schedule. Although each pattern has advantages and disadvantages, it must meet the mining goal in a safe and cost-effective manner. This can be accomplished by looking into the relationship between stoping patterns and ground-related problems. The planning stage defines the period between the beginning of the feasibility study and the onset of mine production. It should be characterized by flexibility to suit any sudden technical changes and market competition. Also, it is of utmost importance to develop a long-term extraction strategy (e.g. plan) that maximizes the overall mine benefits from the ore reserve (**Kazakidis, 2001**; **Kazakidis and Scoble, 2003**; **Mayer and Kazakidis, 2007**; **Musingwini et al., 2007** and **Fuykschot, 2009**). Unplanned mining sequences pose a serious hazard to mining operations' profitability and efficiency. Subsequently, unexpected consequences may have disastrous effects (**Kumral and Sari, 2017**; **Furtado e Faria et al., 2021**). Generally, the mining sequences are designed according to the characteristics of the orebody (e.g. nature, geometry, grade, quantity/reserve, etc.), the quality of the rock mass (e.g. strength, presence of joints, etc.), operational costs (e.g. net present value, volume of mine development works, support system, etc.) and the conditions of the mine environment (e.g. stresses, seismicity, etc.). Such sequences/plans show the mining front and stope extraction order throughout the overall ore deposits. Therefore, these factors have to be included into the designed plan to fulfill the following targets (**Ghasemi, 2012**):

Corresponding author: Wael Abdellah
e-mail address: waelabdellah@aun.edu.eg

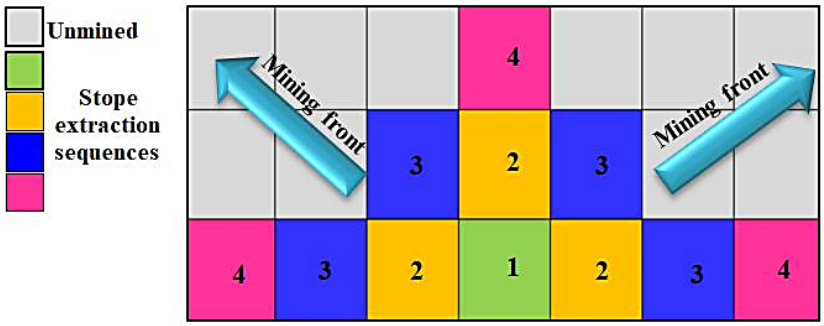

Figure 1: Pillarless mining sequence, centre-out extraction (**Morrison, 1995**)

1. Maximum rate of production (e.g. maximize the economic returns);
2. Minimal operating costs (e.g. least mine development works and preparation time);
3. Manage, control and mitigate ground control hazards (e.g. in-situ stresses, seismicity, ground failure, rock bursts, etc.).

In deep underground mines, it is imperative to extract stopes using a pre-determined pattern to overcome the stress concentration close to unmined stopes/blocks. Failure to develop suitable mining sequences may lead to serious hazards to personnel, damage to machinery, extra expenditures of rehabilitation and installation of rock support and loss of ore reserve (e.g. due to ground failure, seismicity and rockburst) (**Vick, 1983**).

1.2. Pillarless, centre-out stoping pattern

The pillarless, centre-out stoping system is commonly practiced in many Canadian mines, such as Garson Mine, Golden Giant Mine and Creighton Mine (**Potvin and Hudyma, 2000**; **Malek et al., 2009**; **Shnorhokian et al., 2015**). This pattern is preferred when extracting steeply dipping ore deposits to avoid overstressed pillars. Hence, it improves the stability (e.g. by eliminating the stress concentration) and increases the rate of ore recovery (**Henning, 1998**; **Zhang and Mitri, 2008**). In addition, the need for secondary stopes is reduced and thus, deformation of the rock mass is minimized (**Morrison, 1995**; **Villaescusa, 2003**; **Trifu and Suorineni, 2009**). More importantly, the seismicity (e.g. amount of released energy) is decreased (e.g. as mining begins from the centre and advances towards the ore shoulders/sides, see **Figure 1**) particularly when a short lift stope is extracted (**Alexander and Fabjanczyk, 1982**; **Bywater et al., 1983**; **Larsson, 2004**; **Sharma, 2015**). Although this mining system is popular, it has many disadvantages, such as the overall mine production primarily depends on the stope cycle time (e.g. blasting, mucking, hauling, backfilling and curing time before extracting adjacent blocks). In addition, the top of the backfilled large stopes collapsed (e.g. due to poor backfill reinforcement and high stress concentration) and is particularly vulnerable when cemented rockfill (e.g. CRF) is adopted. Consequently, drilling, blasting and dilution issues existed when mining advanced towards adjacent unmined blocks. This problem could be resolved by replacing CRF with hydraulic fill, but this is expensive and time consuming.

2. Drift instability assessment criterion

The serviceability of a mine haulage drift is examined using the Mohr-Coulomb yield-based criterion. Such a criterion is a built-function in most finite element codes when elasto-plastic computation is conducted. The yielding occurs when the rock is loaded past its elastic limit. Therefore, yielding will be considered a measure for drift instability if it extends beyond a certain depth into a rock mass around a haulage drift. According to the applied rule of thumb herein, the resin grouted rebar can sustain 1-ton of axial load per 1-inch anchorage/embedment length of the rockbolt (**Abdellah et al., 2012; Elrawy et al., 2020**). For the purpose of this analysis, it is assumed that the resin grouted rebar (e.g. tensile capacity of 12 tons) installed into drift sidewalls and floor requires at least 12 inches (e.g. 30 cm) of resin anchorage, and the rebar installed into the drift back/roof (e.g. tensile capacity of 24-tons) requires 24 inches (e.g. 60 cm) of anchorage to achieve full-design strength. Based on the support system practiced in most Canadian mines, the lengths of primary supports installed on the sidewalls and floor are 6-ft. (e.g. 1.80 m) and those installed on the roof are 7-ft. (e.g. 2.1 m) for openings of width ≤18 ft. (e.g. 5.5 m). Consequently, an unsatisfactory performance of the drift occurs when the extent of the yield zones exceeds 1.5 m because insufficient anchorage length is available beyond the yield zone. Alternatively, the performance of the drift is considered unsatisfactory if the anchorage length of the rock support installed into the drift sidewalls and floor <30 cm and one installed into the drift back <60 cm.

3. Numerical modelling set up

The analysis has been conducted using two-dimensional finite-element code, RS²D (**Rocscience Inc. RS2,**

Table 1: Mohr-Coulomb model input parameters (**Abdellah et al., 2012**)

Property	Hanging wall (HW)	Footwall (FW)	Ore/stope	Backfill (BF)
γ, MN/m3	0.02782	0.02961	0.04531	0.02
UCS, MPa	90	172	90	3
E, GPa	25	40	20	0.1
Poisson's ratio, υ	0.25	0.18	0.26	0.30
Cohesion, C, MPa	4.80	14.13	10.2	1
Tensile strength, σt, MPa	0.11	1.52	0.31	0.01
Friction Angle, ϕ, deg.	38	42.5	43	30
Dilation angle, φ, deg.	9	10.6	11	0

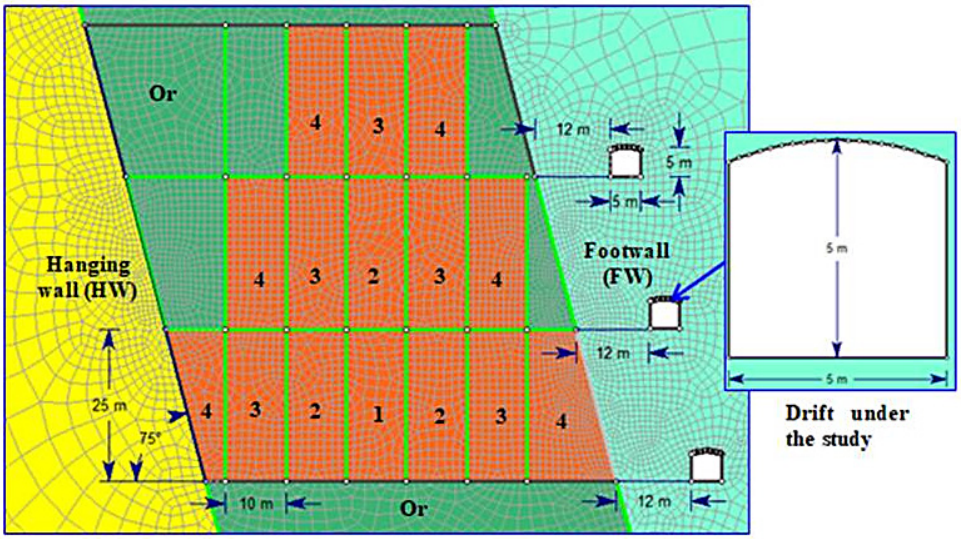

Figure 2: Modelled stopes' geometry and meshing presenting the pyramidal shape of mining sequences

Table 2: Pyramidal pattern mining, stages and number of stope extracted at once

Mining stage	Stope(s) No.	Number of stopes extracted together
1	-	Excavate drifts
2	#1	1
3	#2	3
4	#3	5
5	#4	6
Sum		15

2016). **Table 1** lists the rock mass and backfill properties used in this study (**Abdellah et al., 2011**). Non-linear elasto-plastic analysis, employing Mohr-Coulomb failure criterion, has been adopted for a steeply dipping orebody (e.g. 750), whereby a planned sequence of 15 stopes over three production levels (1175, 1200 and 1225) is simulated in the form of 4 mine-and-fill numerical model steps, as depicted in **Figure 2** and listed in **Table 2**. While doing so, the extent of yield zones is monitored and measured around the haulage drift situated on level 1200.

4. Results and discussion

As stated earlier, rock-soil software, RS^{2}D, has been employed to perform this numerical modelling analysis. The stability of the haulage drift is evaluated in terms of the extent of failure zones into the rock mass based on the length of the rock primary support. The tonnage of unmined ore and the quantity of fill material are then calculated with respect to the mining step. The next sub-section presents the development of plastic zones around the mine haulage drift located at level 1200 (e.g. middle drift).

4.1. Extent of yielding zones around drift

Figure 3 depicts the development of yielding zones around mine haulage drifts at various mining stages/sequences. It can be shown that, the extent of yielding zones increases as mining advances. For instance, the yielding zones extend beyond the anchorage length of rock support (e.g. >1.5m) in the drift left wall (LW) after mining step 4; in the drift right wall (RW) and floor after mining step 5, and in the drift back (roof) after mining step 3.

The progression of yielding zones with respect to mining sequences is listed in **Table 3**, and plotted as well

Table 3: Extents of yielding zones around the middle haulage drift

Mining stage	Extent of yielding zones, m			
	Roof	Floor	Right wall (RW)	Left wall (LW)
1	1.42	0.29	0.30	0.53
2	1.44	0.41	0.39	0.67
3	1.55	0.50	0.44	1.16
4	1.66	0.70	1.45	2.28
5	4.82	2.57	1.88	13.0

in **Figure 4**. It can be seen that the roof of the haulage drift begins to deteriorate at an early stage (e.g. after mining step #3). Also, the rock mass around the left wall (LW) of the haulage drift starts to significantly fail after mining step #4 (e.g. the same mining level; 1200 level). Thus, the same mining level (e.g. 1200 level; where the middle drift stands) is more crucial than the lower (e.g. 1225 level) and upper (e.g. 1175 level) mining levels. The stability of the drift right wall (RW) and the floor deteriorates in the final mining stage (e.g. step #5). Thus, the drift requires secondary support in the roof before mining step #3; before mining step #4 in the left wall (LW) and before mining step #5 in the floor and the right

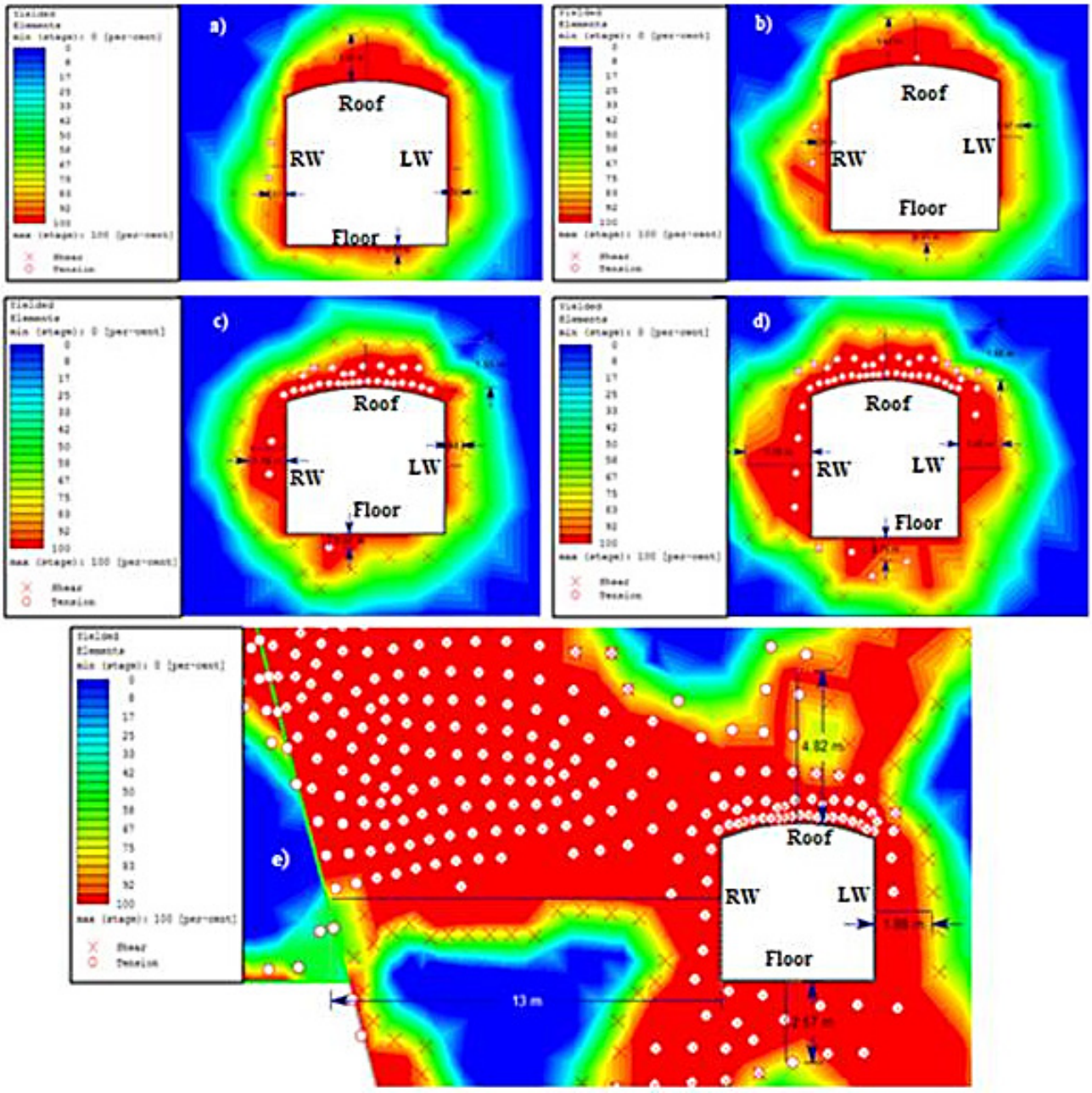

Figure 3: Progression of failure zones around the middle haulage drift at various mining stages a) after excavating the middle drift; b) after excavating stope #1; c) after excavating stopes #2; d) after excavating stopes #3 and e) after excavating stopes #4

wall (RW). The spread of failure zones into the rock mass around unmined stopes is presented and discussed in the next section.

4.2. Extent of yielding zones around unmined stopes

Figure 5 shows the extent of yielding zones into the rock mass of unmined stopes at different mining stages.

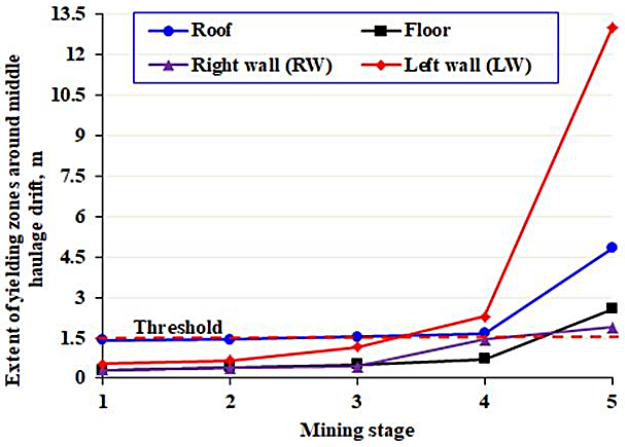

Figure 4: Extent of yielding zones vs. mining stage/sequence

It can be shown that the extent of failure zones spreads as mining progresses. Alternatively, the volume of ore at risk (e.g. unmined stopes) increases as mining proceeds. The next section presents the methodology and assumptions in the calculation of ore at risk at various mining stages.

4.3. Calculation of tonnage of unmined ore at risk

In the following section, the calculation methodology for the tonnage of unmined ore at risk will be introduced with all the assumptions that have been considered. The dimensions of all modelled stopes are fixed (e.g. 10×25m: width×height), see **Figure 2**. The projected depth of ore in the third dimension is taken as unity (e.g. since only two-dimensional analysis is carried out in this study). The following **Equations 1, 2** and **3** are then employed, with the aid of **Figure 5**, to estimate the tonnage of unmined ore at risk.

$$V = H \times W \times L \quad (1)$$

Where:

V: volume of failed/collapsed ore in the roof, floor or sidewalls of unmined stope(s) with respect to mining se-

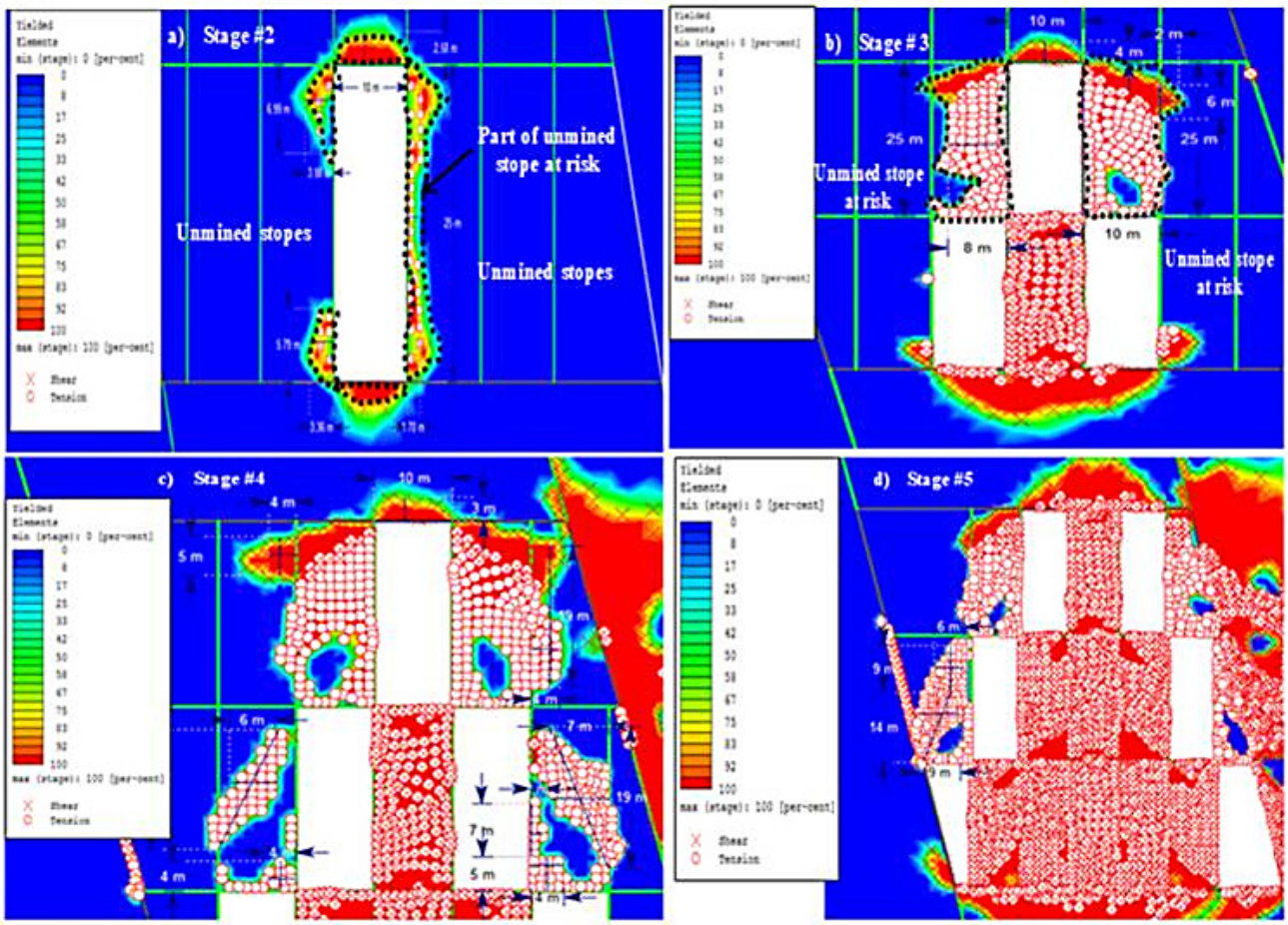

Figure 5: Spread of yielding zones into the rock mass (unmined stopes) at various mining stages a) after extracting stope 1 (step #2) b) after extracting stopes 2 (step #3) c) after extracting stopes 3 (step #4) d) after extracting stopes 4 (step #5)

Table 4: Total volume and tonnage of expected ore to be extracted and amount of unmined ore at risk

Mining Step	No. stope(s) to be mined-out (N)	Stope dimensions (H × W × L), m³	Volume of extracted ore, m³	Tonnage of extracted ore, tons $\left(\gamma = 4.531\ {}^{t}/_{m^3}\right)$	Volume of unmined ore (at risk), m³	
1	-	-	-	-	-	-
2	1	25 × 10 × 1	250	1132.75	115.574	523.67
3	3		750	3398.25	502	2274.56
4	5		1250	5663.75	905	4100.555
5	6		1500	6796.50	632.4	2865.4044
Sum	**15**	**250**	**3750**	16991.25	2154.974	9764.1894

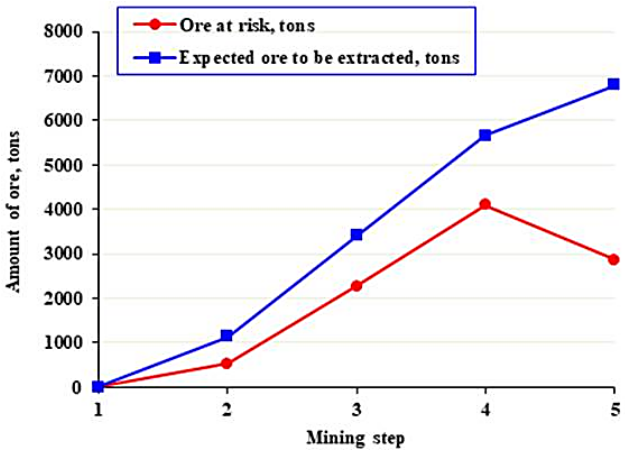

Figure 6: Amounts of ore to be extracted and at risk at various mining step

quences (e.g. estimated from extension of yielding zones into unmined stopes/blocks);

H: height of failed ore in unmined stope(s);

W: width of failed ore in unmined stope(s); and

L: projected depth of failed ore in unmined stope(s) in the third dimension (e.g. it is assumed that L=1 m).

The total volume of ore at risk from an unmined stope (e.g. roof, floor, right wall and left wall) is given from **Equation** (**2**) below:

$$V_T = V_{roof} + V_{floor} + V_{RW} + V_{LW} \quad (2)$$

Where:

V_T: total volume of ore at risk (ore not mined yet);

V_{roof}: volume of failed ore around the crown/back of the unmined stope;

V_{floor}: volume of failed ore around floor of the unmined stope;

V_{RW}: volume of failed ore around the right wall of the unmined stope; and

V_{LW}: volume of failed ore around the left wall of the unmined stope.

The total tonnage of ore at risk, due to rock mass yielding, into an unmined stope(s) is given from Equation (3):

$$T_{at\ risk} = V_T \times \gamma \quad (3)$$

Where:

$T_{at\ risk}$: tonnage of unmined ore at risk with respect to the mining step; and

γ: unit weight of orebody, see **Table** (**1**) (e.g. $\gamma = 0.04531 MN/m^3 = 4531\ kg/m^3 = 4.531 t/m^3$).

By applying the previous **Equations 1**, **2** and **3**, with the aid of **Figure 5a**, to estimate the tonnage of unmined ore at risk after excavating stope #1 (e.g. mining step #2) as follows:

$$V = H \times W \times L$$

$V_{roof} = (2.58 \times 10 \times 1) = 25.8\ m^3$

$V_{RW} = (1.70 \times 25 \times 1) = 42.5\ m^3$

$V_{LW} = (5.79 \times 3.36 \times 1) + (6.99 \times 3.98 \times 1) =$
$= 19.4544 + 27.8202 = 47.2746\ m^3$

Please note that the volume of ore at risk around the floor of unmined stope(s) is not considered only in this mining stage as there is no mining going below stope #1. Thus, the total volume of ore at risk after extraction in stope #1 (e.g. mining step #2) is given as follows:

$V_T = V_{roof} + V_{floor} + V_{RW} + V_{LW} =$
$= V_T = 25.8 + 42.5 + 47.274 = 115.574\ m^3$

Consequently, the tonnage of ore at risk after mining step #2 (e.g. after extracting stope #1) is estimated using **Equation 3** as follows:

$T_{(at\ risk)} = V_T \times \gamma = 115.574 \times 4.531\ t/m^3 = 523.67$ tons

On the other hand, the expected tonnage of ore to be extracted from stope #1 (e.g. after mining step #2) is calculated as follows:

$T = V_T \times \gamma = (W \times H \times L) \times \gamma = (10 \times 25 \times 1)\ m^3 \times$
$\times 4.531\ t/m^3 = 1132.75$ tons

The tonnage of unmined ore at risk after excavating stopes #2 (e.g. mining step #3) is calculated as follows:

In this stage (e.g. mining step #3), three stopes numbered #2 will be extracted. As shown in **Figure 5b**, two complete stopes (e.g. stopes #3) will fail in the same mining level where the middle haulage drift is situated as part of stopes #4 as follows:

$T_{(at\ risk)} = ((10 \times 25 \times 1) + (8 \times 25 \times 1) + (2 \times 6 \times 1) +$
$+ (4 \times 10 \times 1)) \times 4.531 = (250 + 200 + 12 + 40) \times 4.531 =$
$= 502 \times 4.531 = 2274.562$ tons.

Table 5: Amount of backfill material required at each mining stage

Mining stage/step	Number of stopes to be filled after mining	Stope(s) dimensions, (H × W × L), m³	Volume of backfill material, m³	Tonnage of backfill material, tons
1	-	25 × 10 × 1	-	-
2	1		250	250 × 0.02=5
3	3		3 × 250 = 750	750 × 0.02=15
4	5		5 × 2500= 1250	1250 × 0.02=25
5	6		6 × 250 = 1500	1500 × 0.02=30
Sum	**15**	**250**	**3500**	**75**

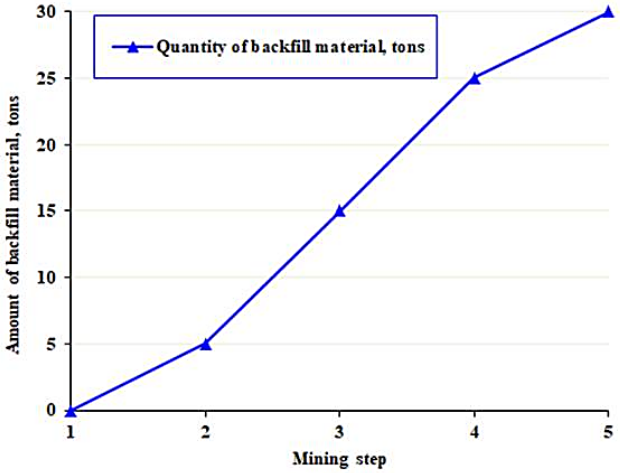

Figure 7: Quantity of backfill material needed to fill extracted stope(s) at different mining stages

The expected tonnage of ore to be extracted during this stage (e.g. mining step #3) is given from:

$T = N \times V_T \times \gamma = (W \times H \times L) \times \gamma = 3$ stopes $\times$

$\times (10 \times 25 \times 1)$ m³ $\times$ 4.531 t/m³ = 3398.25 tons.

The tonnage of unmined ore at risk after excavating stope #3 (e.g. mining step #4) is calculated as follows:

In this stage (e.g. mining step #4), five stopes numbered #3 will be extracted. As shown in **Figure 5c**, two complete stopes (e.g. stopes #3) will fail in addition to several parts of the adjacent stopes #3. The total tonnage of ore at risk after mining step #4 is given from:

$T_{(at\ risk)} = (2\text{stopes} \times (10 \times 25 \times 1) + 2 \times (4 \times 5 \times 1) +$

$+ (10 \times 3 \times 1) + (4 \times 19 \times 1) + (4 \times 4 \times 1) + (7 \times 19 \times 1) +$

$+ (6 \times 16 \times 1) + (7 \times 2 \times 1)) \times 4.531 =$

$= [500+40+30+76+16+133+96+14] \times 4.531 =$

$= 905 \times 4.531 = 4100.555$ tons.

The expected tonnage of ore to be extracted during this stage (e.g. mining step #4) is given from:

$T = N \times V_T \times \gamma = (W \times H \times L) \times \gamma = 5$ stopes $\times$

$\times (10 \times 25 \times 1)$ m³ $\times$ 4.531 t/m³ = 5663.75 tons.

Tonnage of unmined ore at risk after mining step #5 can be calculated as follows:

$T_{(at\ risk)} = (2\text{stopes} \times (10 \times 25 \times 1) + (14 \times 9 \times 1) +$

$+ (9 \times 6 \times 1) + (8.096 \times 25 \times 1)) \times 4.531 = 632.4 \times$

$\times 4.531 = 2865.4044$ tons.

The expected tonnage of ore to be extracted during this stage (e.g. mining step #4) is given from:

$T = N \times V_T \times \gamma = (W \times H \times L) \times \gamma = 6$ stopes $\times$

$\times (10 \times 25 \times 1)$ m³ $\times$ 4.531t/m³ = 6796.5 tons.

Table 4 summarizes the previous calculations for the amount of ore at risk and the expected ore to be extracted at various mining stages. The amount of ore to be extracted and that at risk are plotted against the mining stage as shown in **Figure 6** below. Ore at risk means ore that is not yet mined-out, but is suffering from instability problems due to mining adjacent stope(s) in earlier or previous stage(s). As shown in **Figure 6**, the amount of ore at risk increases as mining advances.

4.4. Quantity of fill material required

The extracted stope(s) should be backfilled before mining the adjacent stope/block(s). Thus, backfill is placed into extracted stope(s) to provide good-confinement to walls and the host rock and to prevent any further rock failure/deformation. Also, it is used to reduce the amount of wastes exposed on the surface. **Table 5** lists the amounts of fill material needed at each mining stage (step), and **Figure 7** displays the amount of fill material at various mining stages. It can be shown that the required amount of backfill material increases as the number of extracted stopes increases. Alternatively, it depends on the ore production/recovery and the dimensions of the extracted stope(s). As introduced before in **Table 1**, the density of the backfill material used in this analysis is 0.02MN/m³ or 2000kg/m³ (2t/m³).

In light of the findings, the Mohr-Coulomb yielding function is the most widely used failure criterion for assessing the stability of subsurface openings as a result of interaction with nearby mining activities. The back (roof) of the mine haulage drift is unstable after mining step 3 based on the findings of this numerical analysis (e.g. failure zones in the rock mass extends beyond the anchorage length of rock support). Alternatively, in the drift roof after mining step 3, the length of rock support anchorage left in the fresh rock mass is less than 30cm. As a result, after mining step 2, it is recommended that an additional rock support be placed in the drift's roof. After mining step 4, the haulage drift's left shoulder (wall) is also affected. As a result, following mining step

3, a more robust rock support is required. Prior to mining step 5, supplemental support may be necessary for both the right shoulder (wall) and the floor of the haulage drift. If there are no mining blocks after step 5, it might not be necessary.

The study reveals that the amount of unmined blocks (e.g. 905m^3 or 4100.56 tons) and backfill material (e.g. 1500m^3 or 30 tons) increase dramatically as a result of the unstable performance of haulage drifts and mining stopes (e.g. more specifically after mining steps 4 and 5 respectively). If the third dimension of the mining stopes, L, (e.g. stope dimensions are H×W×L: 25×10×12 m) is taken into account in three-dimensional analysis, the volume of ore at risk (e.g. 905 m^3) and backfill material (e.g. 1500 m^3) will increase by 12 times. This length, L, was assumed to be equal unity (e.g. L =1 m) for the purposes of two-dimensional analysis.

5. Conclusions

Stope sequencing has a crucial effect on the stability of orezone access units (e.g. haulage drifts), unmined blocks and host rock. A pyramidal stoping pattern (e.g. pillarless, centre-out) has been implemented in this numerical analysis to extract 15 stopes over three production levels (e.g. 1175, 1200 and 1225) into 4 mine-and-fill stages. While doing so, the performance of mine haulage drift is monitored and evaluated based on the spread of yielding regions into rock mass surrounding drift. Consequently, the performance of haulage drift is considered unsatisfactory if the extent of yielding zones exceeds the minimum embedment (anchorage) length of rock primary support. For the purpose of this study, the threshold of the anchorage length of rockbolts installed in the drift sidewalls and floor is 12-inches or 30cm (e.g. for bolts of 1.80m long) and for those installed in the drift back is 24-inches or 60 cm (e.g. for bolts of 2.1m long). Alternatively, if the length of yielding zones exceeds 1.5m (e.g. anchorage length <30 cm for bolts of 1.80m long and <60 cm for bolts of 2.10m long), then the drift performance is not acceptable (unsatisfactory). In addition, the amount of ore at risk (e.g. estimated from unmined stopes) and the required quantity of fill material are calculated and discussed at various mining steps. The results reveal that, as mining progresses, the stability of the haulage drift deteriorates and the amount of unmined ore at risk and the required quantity of fill material increase.

Three-dimensional analysis is advised in order to accurately depict real mine geometry (e.g. stope third dimension) and assess the extent of yielding zones into the third dimension. It's also a good idea to try out different stoping options (scenarios) and assess how stable and productive they are (e.g. amount of ore extracted and that is not yet mined-out or still under risk). Field measurements must be used to check and validate the numerical results (e.g. stresses, deformations).

Acknowledgements

The author wishes to thank RocScience for providing him with a valid licence for the RS^{2}D programme. Their help is much appreciated by the author. The reader is directed to the following URL for further information on RS^{2}D software: https://www.rocscience.com/rocscience/products/rs2d

6. References

Abdellah, W., Mitri, H. and Thibodeau, D. (2012): Stochastic evaluation of haulage drift unsatisfactory performance using random Monte-Carlo simulation. Int. J. Mining and Mineral Engineering 4, 1, 63-87. DOI:10.1504/IJMME.2012.048000

Alexander, E. G. and Fabjanczyk, M. W. (1982): Extraction design using open stopes for pillar recovery in the 1100 orebody at Mount Isa. Proc. Design and Operations of caving and Sublevel Stoping Mines, Stewart (ed.), SME, 437-445.

Appianing, E. J. A., and Ben-Awuah, E. (2018): Underground Mining Stope Layout Optimization and Production Scheduling: A Review of Existing Solvers and Algorithms. MOL Report Nine, 271-304.

Brickey, A. J. (2015): Underground production scheduling optimization with ventilation constraints. Colorado School of Mines, United States. Brickey_mines_0052E_10785.pdf

Bywater, S., Cowling, R. and Black, B. N. (1983): Stress measurements and analysis for mine planning. Paper presented at the 5th ISRM Congress, Melbourne, Australia, April 1983.Paper Number: ISRM-5CONGRESS-1983-112

Carpentier, S., Gamache, M. and Dimitrakopoulos, R. (2016): Underground long-term mine production scheduling with integrated geological risk management. Transactions of the Institution of Mining and Metallurgy, Section A: Mining Technology 125(2), 1743286315Y.000. DOI:10.1179/1743286315Y.0000000026

De Santis, F., Contrucci, I., Kinscher, J., Bernard, P., Renaud, V., and Gunzburger, Y. (2019): Impact of Geological Heterogeneities on Induced-Seismicity in a Deep Sublevel Stoping Mine. Pure and Applied Geophysics. 176, 697–717. https://doi.org/10.1007/s00024-018-2020-9

Elrawy, W. A., Abdelhaffez, G. S. and Saleem, H. A. (2020): Stability assessment of underground openings using different rock support systems. Rudarsko-geološko-naftni zbornik (The Mining-Geological-Petroleum Engineering Bulletin), 35, 1, 49-64. DOI: 10.17794/rgn.2020.1.5

Forbes, B., Vlachopoulos, N., Diederichs, M. S., Hyett, A. J. and Punkkinen, A. (2020): An in situ monitoring campaign of a hard rock pillar at great depth within a Canadian mine. Journal of Rock Mechanics and Geotechnical Engineering, 12, 427-448. https://doi.org/10.1016/j.jrmge.2019.07.018

Furtado e Faria, M., Dimitrakopoulos, R. and Pinto, C. (2021): Stochastic stope design optimisation under grade uncertainty and dynamic development costs, International journal of mining, reclamation and environment. https://doi.org/10.1080/17480930.2021.1968707

Fuykschot, J. (2009): Strategic Mine Planning Flexible mine planning to meet changes in the business environment. SRK consulting, Minex Conference.

Ghasemi, Y. (2012): Numerical studies of mining geometry and extraction sequencing in Lappberget, Garpenberg. Lulea University of Technology, Sweden, 116 p. diva2: 1030651

Henning, J. G. (1998): Ground control strategies at the bousquet 2 mine. McGill University, Canada, 129 p. https://escholarship.mcgill.ca/concern/theses/wd375z59b

Kazakidis, V. N. (2001): Operatin risk: Planning for flexible mining systems. University of British Columbia, Canada. http://hdl.handle.net/2429/13125

Kazakidis, V. N. and Scoble, M. J. (2003): Planning for Flexibility in Underground Mine Production Systems. Mining Engineering, 55(8), 33-38.

Kumral, M., and Sari, Y. A. (2017): Simulation-based mine extraction sequencing with chance constrained risk tolerance, Simulation: Transactions of the Society for Modeling and Simulation International 93(6), 527-539. doi: 10.1177/0037549717692415

Larsson, K. (2004): Seismicity in Mines- A review. Technical Report, Luleå University of Technology, 2004:22 - ISSN: 1402-1536 - ISRN: LTU-TR--04/22—SE.

Malek, F., Suorineni, F. T. and Vasak, V. (2009): Geomechanics Strategies for Rockburst Management at Vale Inco Creighton Mine. ROCKENG09: Proceedings of the 3rd CANUS Rock Mechanics Symposium, Toronto, Canada. Ed: Diederichs, M. and Grasselli, G.

Mayer, Z. and Kazakidis, V. (2007): Decision Making in Flexible Mine Production System Design Using Real Options. Journal of construction engineering and management, 133, 2, 169-180. DOI:10.1061/(ASCE)0733-9364(2007) 133:2(169)

Morrison, D. (1995): Fragmentation – the future. EXPLO 95 Conference, Australasian Institute of Mining and Metallurgy (AusIMM), Brisbane, Australia, September 1995

Musingwini, C., Minnitt, R. C. A. and Woodhall, M. (2007): Technical operating flexibility in the analysis of mine layouts and schedules. The Journal of The Southern African Institute of Mining and Metallurgy (SAIMM), 107, 129-136.

Potvin, Y. and Hudyma, M. (2000): Open stope mining in Canada. Procc MassMin 2000, Australasian Institute of Mining and Metallurgy (AustIMM), Brisbane, Australia.

RocScience Inc. (2016): Rock and Soil 2-dimensional analysis program (RS^2D). https://www.rocscience.com/software/rs2.

Sharma, V. (2015): Long-term schedule optimization of an underground mine under geotechnical and ventilation constraints using sot, Laurentian University, Canada. https://zone.biblio.laurentian.ca/dspace/handle/10219/2310

Shnorhokian, S., Mitri, H. and Moreau-Verlaan, L. (2015): Stability assessment of stope sequence scenarios in a diminishing ore pillar. International Journal of Rock Mechanics and Mining Sciences (IJRMMS), 74, 103-118 . https://doi.org/10.1016/j.ijrmms.2014.12.005

Trifu C. I. and Suorineni, F. T. (2009). Use of microseismic monitoring for rockburst management at Vale Inco mines. Proceedings of 7th International Symposium on Rockburst and Seismicity in Mines (RASIM7). New York.

Vick, S. G., (1983): Planning, design and analysis of tailings dams, Toronto, ON, Canada: Wiley-Interscience. http://hdl.handle.net/2429/76455

Villaescusa, E. (2003): Global extraction sequences in sublevel stoping. MPES 2003 Conference, Kalgoorlie.

Wu, J. (2020): Research on sublevel open stoping recovery processes of inclined medium-thick orebody on the basis of physical simulation experiments. PLoS ONE 15(5): e0232640. https:// doi.org/10.1371/journal.pone.0232640

Yao, M., Sampson-Forsythe, A. and Punkkinen, AR. (2014): Examples of ground support practice in challenging ground conditions at Vale's deep operations in Sudbury. Proceedings of the seventh International Conference on Deep and High Stress Mining, Australian Centre for Geomechanics, Perth, pp. 291-304. https://doi.org/10.36487/ACG_rep/1410_19_Yao

Zhang, Y. and Mitri, H. S. (2008): Elastoplastic stability analysis of mine haulage drift in the vicinity of mined stopes. International Journal of Rock Mechanics & Mining Sciences 45 (4), 574–593. https://doi.org/10.1016/j.ijrmms.2007.07.020

SAŽETAK

Utjecaj otkopavanja komora bez stupova redoslijedom od centra prema van na stabilnost transportnih hodnika i količinu nestabilne rude

Uzimajući u obzir redoslijed otkopavanja, svrha je ovoga članka istražiti utjecaj otkopavanja bez sekundarnih stupova, primjenjujući piramidalni niz otkopavanja od centra prema van, na stabilnost transportnih hodnika, na količinu neotkopane nestabilne rude u komorama i potrebnu količinu materijala za zapunjavanje. Za procjenu stabilnosti transportnih hodnika te procjenu količine neotkopane i nestabilne rude uslijed rudarskih aktivnosti primijenjena je širina plastične zone deformacija unutar stijenske mase oko transportnih hodnika i neotkopanih komora. Rezultati su prikazani i raspravljeni u smislu veličine zone sloma, količine nestabilne sirovine u neotkopanim blokovima i količine potrebnoga materijala za zapunjavanje ovisno o fazi iskopavanja. Ispitivanjima je ustanovljeno da se stabilnost transportnih hodnika naglo smanjuje. Do sloma svoda transportnoga hodnika dolazi u ranoj fazi (nakon 3. koraka otkopavanja). U svodu hodnika, lijevome zidu, podu i desnome zidu, zone sloma izmjerene su na 1,55 m (korak 3), 2,28 m (korak 4), 2,57 m (korak 5) i 1,88 m (korak 5). Nakon 4. koraka iskopavanja, izračunano je ukupno 905 m^3 neotkopane nestabilne rude (4100 tona). Pri tome je u 5. koraku otkopavanja potrebno ukupno 1500 m^3 (30 tona) materijala za zapunjavanje i ojačavanje komora.

Ključne riječi
stabilnost transportnoga hodnika, nestabilna ruda, količina materijala za zapunjavanje, opkopavanje bez stupova od centra prema van, zona plastičnih deformacija

Author contribution

Wael R. Abdellah (Associate Professor, Mining Engineering, University of Assiut, Egypt) has conducted all numerical modelling, interpreted the results, and wrote the entire draft and revised manuscript.